Journal of Hazardous Materials 172 (2009) 99–107

Contents lists available at ScienceDirect

Journal of Hazardous Materials

journal homepage: www.elsevier.com/locate/jhazmat

Adsorption kinetics and isotherm of anionic dyes onto organo-bentonite from single and multisolute systems

Dazhong Shen[a,*], Jianxin Fan[a], Weizhi Zhou[b], Baoyu Gao[b], Qinyan Yue[b], Qi Kang[a]

[a] School of Chemistry, Chemical Engineering and Material Science, Shandong Normal University, Jinan, 250014, PR China
[b] School of Environmental Science and Environmental Engineering, Shandong University, Jinan, 250100, PR China

ARTICLE INFO

Article history:
Received 12 September 2008
Received in revised form 23 June 2009
Accepted 24 June 2009
Available online 3 July 2009

Keywords:
Adsorption isotherm
Kinetics
Mixed dyes
Organo-bentonite
Polyelectrolyte

ABSTRACT

The performances of polydiallydimethylammonium modified bentonite (PDADMA–bentonite) as an adsorbent to remove anionic dyes, namely Acid Scarlet GR (AS-GR), Acid Turquoise Blue 2G (ATB-2G) and Indigo Carmine (IC), were investigated in single, binary and ternary dye systems. In adsorption from single dye solutions with initial concentration of 100 μmol/L, the dosage of PDADMA–bentonite needed to remove 95% dye was 0.42, 0.68 and 0.75 g/L for AS-GR, ATB-2G and IC, respectively. The adsorption isotherms of the three dyes obeyed the Langmuir isotherm model with the equilibrium constants of 0.372, 0.629 and 4.31 L/μmol, the saturation adsorption amount of 176.3, 149.2 and 228.7 μmol/g for ATB-2G, IC and AS-GR, respectively. In adsorption from mixed dye solutions, the isotherm of each individual dye followed an expanded Langmuir isotherm model and the relationship between the total amount of dyes adsorbed and the total equilibrium dye concentration was interpreted well by Langmuir isotherm model. In the region of insufficient dosage of PDADMA–bentonite, the dye with a larger affinity was preferentially removed by adsorption. Desorption was observed in the kinetic curve of the dye with lower affinity on PDADMA–bentonite surface by the competitive adsorption. The kinetics in single dye solution and the total adsorption of dyes in binary and ternary dye systems nicely followed pseudo-second-order kinetic model.
© 2009 Elsevier B.V. All rights reserved.

1. Introduction

Dyes are important water pollutants which are generally present in the effluents of the textile, leather, food processing, dyeing, cosmetics, paper, and dye manufacturing industries. Over 10^5 commercially available dyes exist and more than 7×10^5 tons are produced annually [1]. Consequently, approximately 7×10^4 tons/year of dyes are discharged into waste streams by the textile industry. Due to intense color they reduce sunlight transmission into water hence affecting aquatic plants, which ultimately disturb aquatic ecosystem. In addition, they are also carcinogenic and possess a serious hazard to aquatic living organisms. As a result, many governments have established environmental restrictions with regard to the quality of colored effluents and have forced dye houses to decolorize their effluents before discharging. Thus, the removal of dyes from effluents before they are mixed up with unpolluted natural water bodies is important. Among the many methods available for the removal of dyes from water namely: adsorption [2–4], oxidation [5–7], biological treatment [8–10], coagulation and flocculation [11–13] and membrane processes [14,15], adsorption process is one of the most efficient methods of removing pollutants from wastewater. The advantages of adsorption process are for its simplicity in operation, inexpensive (compared to other separation processes) and without sludge formation. The most commonly used adsorbent in industrial wastewater treatment systems is activated carbon because it has a large specific surface area, although it is a bit expensive to run such systems [16]. Studies indicated that many materials, such as chitosan [17], bagasse pith [18], peanut hull [19], peat [20], rice husk [21], fly ash [22], wood sawdust [23], natural clays including bentonite [24], montmorillonite [25], alunite [26], sepiolite [27], zeolite [28], diatomite [29] and hydrotalcite [30] were used as adsorbents which could effectively remove the dyes from wastewaters.

Bentonite is the commercial designation of a natural clay mineral, the main component of which is montmorillonite. Bentonite is widely used as adsorbent due to its high specific surface area. Na^+–bentonite carries a permanent negative charge in its structural framework and has little affinity for the anionic dyes. Previous studies show that the modified bentonite obtained by replacing the inherent clay inorganic cations with suitable quaternary amine cations or surfactant can affect the capacity of the bentonite to remove organic contaminants from aqueous solution [31–34]. There has been much interest in the use of organo-bentonites as adsorbents to prevent and remediate environmental contamination by dyes and other organic pollutants [35–41].

* Corresponding author. Tel.: +86 0531 86180740; fax: +86 0531 82615258.
E-mail address: dzshen@sdnu.edu.cn (D. Shen).

0304-3894/$ – see front matter © 2009 Elsevier B.V. All rights reserved.
doi:10.1016/j.jhazmat.2009.06.139

Nomenclature

$\boldsymbol{A}$	absorbance matrix
$\boldsymbol{C}$	concentration matrix
C	residual liquid concentrations of dye (mol/L)
C_e	liquid phase dye concentration at equilibrium (mol/L)
C_0	initial liquid concentrations of dye (mol/L)
h	initial rate of adsorption (mol/g min)
k_1	equilibrium rate constant of pseudo-first-order sorption (min^{-1})
k_2	equilibrium rate constant of pseudo-second-order sorption (g/mol min)
$\boldsymbol{K}$	absorptivity coefficient matrix
K_L	Langmuir isotherm constant (L/mol)
$\boldsymbol{K}^T$	the transpose of $\boldsymbol{K}$ matrix
m	mass of adsorbent used (g)
Q_e	amount of dye adsorbed at equilibrium (mol/g)
Q_{e1}	equilibrium adsorption amount in pseudo-first-order kinetic model (mol/g)
Q_{e2}	equilibrium adsorption amount in pseudo-second-order kinetic model (mol/g)
Q_j	amount of dye adsorbed at contact time t (mol/g)
Q_{max}	maximum adsorption capacity of the adsorbent (mol/g)
R_L	dimensionless equilibrium parameter
R^2	linear correlation coefficient
t	contact time (min)
V	volume of dye solution (L)

In the application of adsorption for purification of wastewater, the solution will normally be a mixture of many compounds rather than a single one. The interactions of these compounds may mutually enhance or mutually inhibit adsorption capacity [42]. However, almost all of these studies were based on single solute systems. The aim of this work is to study the adsorption of dyes onto organo-bentonite from multi-component systems. To study the adsorption behavior of dye mixtures, it is necessary to determinate simultaneously the concentrations of various dyes in the sample. By using a multiple linear regression (MLR) method, the residual concentrations of dyes in the mixture were evaluated from the spectrometric data. On the other hand, the influence of light scatter from residual particles in supernatants on the concentration determination of solutes can be corrected [43,44].

In this work, the adsorption of anionic dyes, namely, Acid Scarlet GR (AS-GR), Acid Turquoise Blue 2G (ATB-2G) and Indigo Carmine (IC), from single dye solutions and multisolute dye solutions onto polyelectrolyte-modified bentonite was investigated. Anionic dyes were chosen as the model system because the overwhelming majority of synthetic dyes currently used are the highly water soluble anionic dyes. These anionic dyes are the most problematic compared to other forms of dyes and must be removed from wastewater. Cationic polymer, polydiallydimethylammonium (PDADMA) was used to modify the surface of bentonite. The kinetics and isotherms for dyes adsorption onto PDADMA-modified bentonite (PDADMA–bentonite) were studied in single, binary and ternary dye solutions.

2. Materials and methods

2.1. Chemicals and materials

The cationic polyelectrolyte, PDADMA (with molecular weight of ca. 1.2×10^6 and charge density of 100%), was produced by Bin Zhou Chemicals Co. (Shandong, China). The commercially available anionic dyes, AS-GR, ATB-2G and IC, were purchased from Shanghai Maikun Chemicals Company, China. The molecular structures of the three dyes and PDADMA are illustrated in Fig. 1. Deionized water was used everywhere in the study. The dye solutions were prepared by dissolving the dyes into deionized water. The pH of the dye solutions was adjusted to a given level by addition HCl or NaOH solution and indicated by a pH meter. Dye solutions with pH 5 were used in all adsorption experiments except in the experiment related to pH effect.

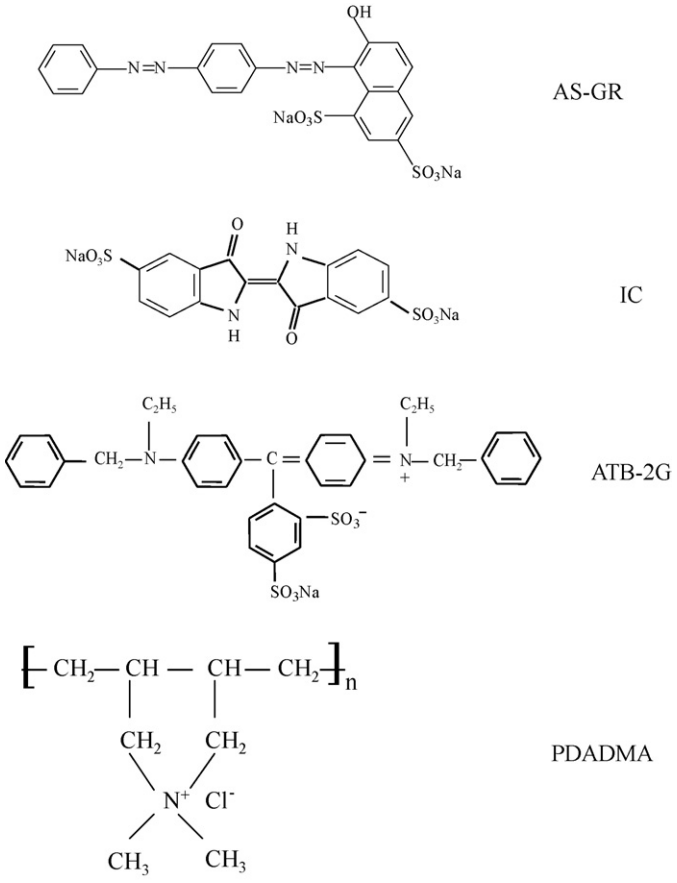

Fig. 1. Structure formula of AS-GR, IC, ATB-2G and PDADMA.

The Na^+-exchanged form of bentonite used in this study was obtained from the city of Weifang in Shandong, China. It contained about 95% montmorillonite with the chemical composition of 69.32% SiO_2, 14.27% Al_2O_3, 1.99% CaO, 2.69% MgO, 1.84% Fe_2O_3, 1.85% Na_2O, 1.38% K_2O as reported by the supplier. The cation exchange capacity of the bentonite (0.67 meq./g) was measured by the methylene blue method [45].

2.2. Preparation of PDADMA–bentonite

Twenty grams of oven-dried bentonite was dispersed into 250 mL water to swell the clay for 30 min. Under stirring, 100 mL of 4% PDADMA solution was added slowly into the slurry of bentonite at 65 °C. Then, the dispersion was stirred at 65 °C for 3 h. The obtained PDADMA–bentonite complex was separated from the mixture by vacuum filtering and washed several times with deionized water. The prepared complex was dried at 80 °C and activated for 1 h at 105 °C in an oven, and then gently crushed, ground and sieved through 300 mesh and stored for further use. The samples were analyzed by X-ray powder diffraction using a Rigaku Dmax

2500 diffractometer with Cu Kα radiation. The X-ray tube was operated at 40 kV and 30 mA beam current.

2.3. Measurements of removal efficiency and isotherm

In the adsorption equilibrium experiments, a pre-selected amount of adsorbent was brought into contact with 200 mL dye solution in a glass bottle. The initial concentration was the same for each individual dye in mixed dye solutions. A series of bottles with consecutively increasing adsorbent dosage were prepared. The bottles were shaken on a reciprocating shaker operated at a room temperature of 25 °C for 4 h to reach adsorption equilibrium. The samples were subjected to centrifugation at 3×10^3 rpm for 15 min. Absorbance spectra of the supernatants were recorded every 1 nm in the range 400–700 nm on a spectrophotometer (Lambda 35, Perkin-Elmer Instrument) using silica cells of path length 1 cm. Deionized water was employed as the blank sample. All the spectra were repeatedly measured five times and the averaged values were recorded. The residual concentration of each dye in the supernatant was estimated from the absorbance spectra by using an MLR analysis method [43]. The principle of MLR method was given by

$$C = (\boldsymbol{K}^{\mathrm{T}}\boldsymbol{K})^{-1}\boldsymbol{K}^{\mathrm{T}}\boldsymbol{A} \quad (1)$$

here $\boldsymbol{A}$, $\boldsymbol{K}$ and $\boldsymbol{C}$ are the matrices of absorbance, absorptivity coefficient and concentration, respectively. $\boldsymbol{K}^{\mathrm{T}}$ is the transpose of the $\boldsymbol{K}$ matrices.

It was noted that the $\boldsymbol{K}$ matrix was constituted by the absorptivity coefficients for each dye and the scattering spectrum of residual particles in solution. The addition of scattering spectrum in $\boldsymbol{K}$ matrix was needed to correct the influence of light scattering on the concentration estimation of adsorbates [44]. The absorptivity coefficients for each dye were determined from the absorbance measurements of the dye at specific concentrations. Calibration curve was then constructed by plotting absorbance of each single dye against dye concentration. The slopes of the linear regression curves gave the absorptivity coefficients for each dye at wavelengths ranged of 400–700 nm. The scattering spectrum was obtained from the PDADMA–bentonite supernatant without dye. The absorbance data at a group (30–40) wavelengths in the range of 400–700 nm were chosen to calculate the unknown dye concentration by Eq. (1). The calculation in MLR analysis method was done with software named Matlab 6.0.

The color removal efficiency of the dye j was calculated as follows

$$\text{Color removal}(\%) = \left(1 - \frac{C_{ej}}{C_{0j}}\right) \times 100 \quad (2)$$

where C_{0j} and C_{ej} are the initial and residual liquid concentrations of the dye j, respectively. The amount of dye j adsorbed at equilibrium, Q_{ej}, was calculated by

$$Q_{ej} = (C_{0j} - C_{ej})\frac{V}{m} \quad (3)$$

where V and m are the liquid volume and the mass of PDADMA–bentonite used, respectively. For each experiment three parallel samples were prepared and tested, only the averaged value was reported here.

2.4. Measurements of adsorption kinetics

Adsorption kinetics study was carried out in order to test the relationship between contact time and dye uptake. Dye solution (400 mL) with initial concentration of 100 μmol/L for each individual dye was prepared. A pre-selected amount of PDADMA–bentonite was dispersed in the dye solution while being constantly stirred by a magnetic stirrer at a speed of 300 rpm. Under stirring, the adsorbent was well dispersed in the dye solution. After a given contact time, 10 mL mixture of dyes and adsorbent was sampled and subjected to centrifugation at 3×10^3 rpm for 15 min. The time interval between the addition of the adsorbent to the start of the centrifugation was recorded as the contact time. As the mixture of adsorbent and dye solution was withdrawn under stirring, the feed ratio of adsorbent to dye was kept constant after sampling though the volume of the mixture was decreased. Hence, a group of 10 mL mixture of adsorbent and dye solution was subsequently withdrawn after pre-selected contact time. The residual concentrations for individual dye in the supernatants were analyzed by the method described above. The amount of dye j adsorbed after a contact time of t, Q_{tj}, was calculated by.

$$Q_{tj} = (C_{0j} - C_{tj})\frac{V}{m} \quad (4)$$

where C_{tj} is the liquid phase concentration of dye j after contact time of t.

3. Results and discussion

3.1. Modification bentonite by polyelectrolyte

Adsorption of anionic dyes onto natural bentonite was limited because both the bentonite surface and the dye molecules had negative charges. To increase the electrostatic attraction and improve the adsorption capacity, the surface of raw bentonite was modified by a cationic polymer (PDADMA). Fig. 2 highlights the XRD powder patterns of bentonite before and after the treatment with PDADMA. In the angle range of 3–9°, the diffraction peaks of bentonite and PDADMA–bentonite occurred at 5.83° and 6.90°, which corresponded to the basal spacings in bentonite and PDADMA–bentonite of 1.28 and 1.51 nm, respectively. The results were likely due to the fact that PDADMA molecules were partially intercalated into the interlayers of bentonite and expanded the interlamellar spacing. Thus, using a cationic polyelectrolyte template realizes electrostatic attraction between the negatively charged SO_3^- anionic groups of dye and quaternary ammonium groups in bentonite layers. In this work, PDADMA–bentonite was used as an adsorbent to remove anionic dyes.

3.2. Effect of pH

The pH of solution from which adsorption occurs may influence the extent of adsorption. In general, initial pH value may enhance

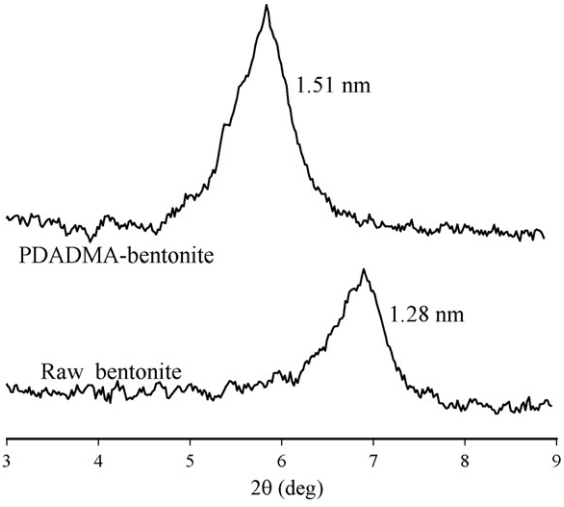

Fig. 2. X-ray diffraction patterns of raw Na–bentonite and PDADMA–bentonite.

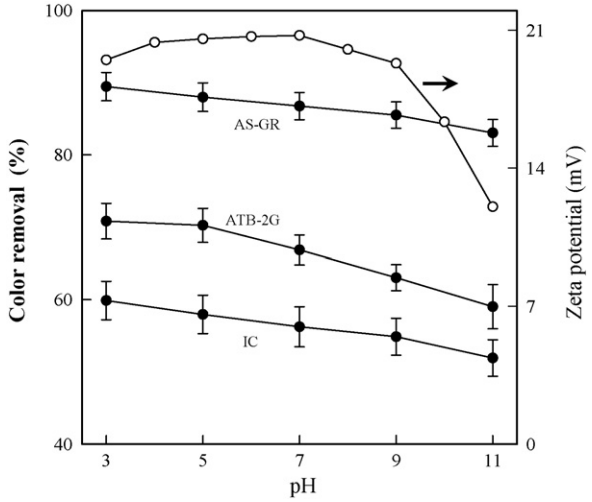

Fig. 3. Effect of the initial solution pH on Zeta potential of PDADMA–bentonite and color removal efficiency of AS-GR, IC and ATB-2G from single dye solutions. The dose of PDADMA–bentonite was 0.4 g/L and the initial dye concentration was 100 μmol/L.

or depress the uptake. Effect of initial pH was investigated in the range of 3–11. In the experiments, the dose of PDADMA–bentonite was 0.4 g/L. Blank studies for AS-GR, IC and ATB-2G were done in the pH range of 3–11. The dye solutions were kept for 1 h after the pH adjustment and, thereafter, the absorbance of the solution was found out. It is found that the color is stable at each pH in the range used. As seen in Fig. 3, the color removal of the three anionic dyes by adsorption onto PDADMA–bentonite reduced slightly with increasing pH from 3 to 11. The surface charge of PDADMA–bentonite was positive in the examined pH range. The higher removal efficiency of the dye by adsorption onto PDADMA–bentonite at low pH values may be due to neutralization of the negative charge at its surface as $-SO_3^-$ anion, which increased the protonation and the electrostatic attraction between the negatively charged $-SO_3^-$ anion and the positively charged adsorption site [46]. In alkaline medium, the Zeta potential of the PDADMA–bentonite reduced with increasing pH. On the other hand, there was competition adsorption between the OH^- ions and the dye anions. Hence, the removal efficiency of the dyes decreased with increasing pH. But still significant amount of color removal was observed as the pH of the solution increased from 7 to 11. This suggested that the chemisorption mechanism may be operative [36]. As the pH values of the dye solutions themselves were in range of 5–6, the initial pH 5 was employed in subsequent adsorption experiments.

3.3. Color removal efficiency in single and mixed dye solutions

To assess the adsorption potential of the prepared PDADMA–bentonite for anionic dyes, the color removal efficiencies were measured in single and mixed dye solutions. As shown in Fig. 4, PDADMA–bentonite exhibited high adsorption efficiency for the three dyes. The removal efficiency followed the predicted pattern of increasing as the dosage was increased. Under our experimental conditions, the dosage of PDADMA–bentonite needed to remove 95% dye from a 100 μmol/L single dye solution was 0.42, 0.68 and 0.75 g/L for AS-GR, ATB-2G and IC, respectively. After that, the removal efficiencies of the three dyes increased slowly and achieved to 99.5% under the dose of 1.2 g/L. It should be noted that the light scattering from the residual particles dispersing in the supernatant causes a positive error in the estimation of the residual concentration of adsorbate in supernatant [43,44]. Without correction of the light scattering effect in spectrometric

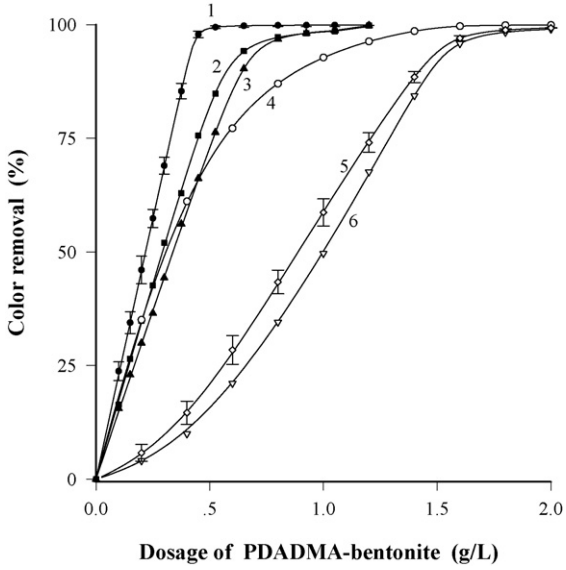

Fig. 4. Effect of the dosage of PDADMA–bentonite on the color removal efficiency of AS-GR, IC and ATB-2G from single and ternary dye solutions. The initial concentration was 100 μmol/L for each dye. (1) AS-GR; (2) ATB-2G; (3) IC; (4) AS-GR in ternary dye mixture; (5) IC in ternary dye mixture; and (6) ATB-2G in ternary dye mixture.

data, the maximum removal efficiency was limited to 96–97% even under the dose of 3 g/L (data were not shown).

As illustrated in Figs. 4 and 5, the removal behavior of the three dyes was different in mixed dye solutions. Comparing with the results in single dye solutions under the same dosage, a reduction in removal efficiency of the individual dye in the mixed dye systems was observed, although the extent of reduction was different among the dyes. Under the dose of adsorbent of 0.4 g/L, for example, the removal efficiency of AS-GR was reduced from 90% (in single solution) to 71% (in binary solution of AS-GR + ATB-2G) and to 61% (in ternary dye solution). But the removal of ATB-2G was reduced from 59% (in single solution) to 19% (in binary solution of AS-GR + ATB-2G) and to 11% (in ternary dye solution). The reduction in removal of IC was larger than that of AS-GR but less than that of ATB-2G. It was revealed that AS-GR was preferen-

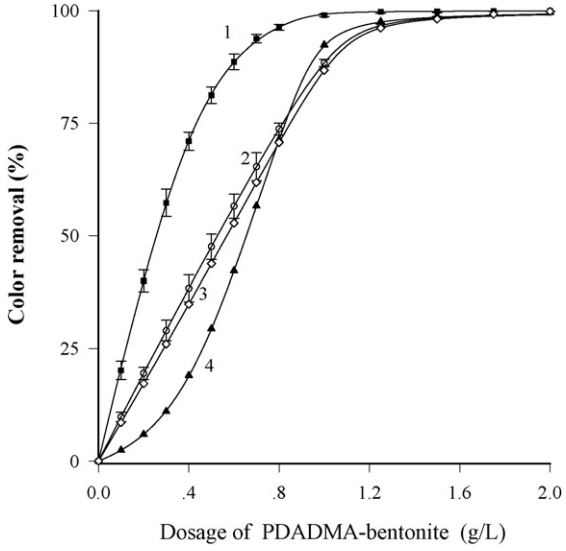

Fig. 5. Effect of the dosage of PDADMA–bentonite on the color removal efficiency of dyes from binary dye solutions. The initial concentration was 100 μmol/L for each dye. (1) AS-GR in AS-GR + ATB-2G; (2) IC in ATB-2G + IC; (3) ATB-2G in ATB-2G + IC; and (4) ATG-2B in AS-GR + ATG-2B.

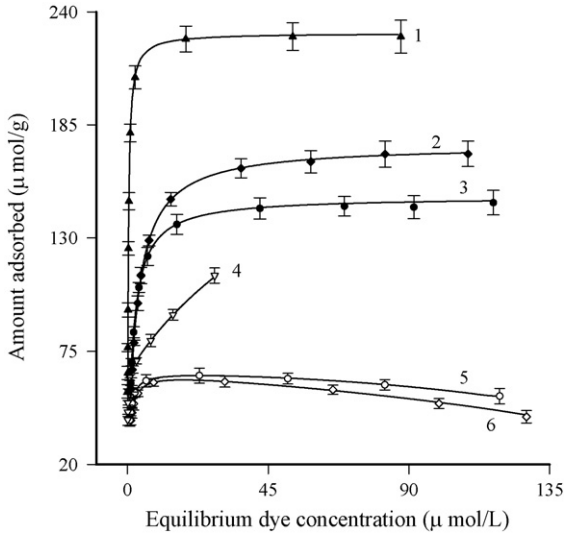

Fig. 6. Adsorption isotherms of AS-GR, IC and ATB-2G onto PDADMA–bentonite from single and ternary dye solutions. The initial concentration was the same for each dye in the ternary mixture. (1) AS-GR; (2) ATB-2G; (3) IC; (4) AS-GR in ternary mixture; (5) IC in ternary mixture; and (6) ATG-2B in ternary mixture.

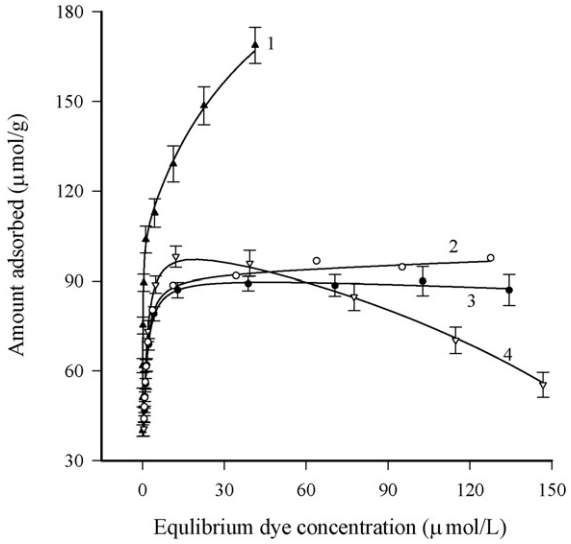

Fig. 7. Adsorption isotherms of AS-GR, IC and ATB-2G onto PDADMA–bentonite from binary dye mixtures with the same initial concentration for each dye. (1) AS-GR in AS-GR + ATB-2G; (2) IC in ATB-2G + IC; (3) ATB-2G in ATB-2G + IC; and (4) ATB-2G in AS-GR + ATB-2G.

tially removed in mixed dye systems, especially in the region of low dose of PDADMA–bentonite. The result indicated a competitive adsorption mechanism. In the case of low dose, the adsorption sites on the PDADMA–bentonite were insufficient to all the dye molecules. AS-GR was preferentially adsorbed in binary solution of AS-GR + ATB-2G due to its larger affinity to the adsorbent. As the dose increased, more and more sites were available for dye adsorption, the competitive adsorption was weakened between AS-GR and ATB-2G. Hence, the adsorption of ATB-2G was speeded and approached to 100% at high dose, too. The ratio of the removal of AS-GR to ATB-2G was decreased from 6.8 (at dose of 0.2 g/L) to 1.001 (at dose of 2.0 g/L). It was worthwhile to note that the removal efficiency of IC and ATB-2G was similar in the binary dye system of IC and ATB-2G. With increasing of the dose from 0.2 to 2.0 g/L, the ratio of the percent adsorption of IC to ATB-2G decreased only from 1.13 to 1.00. The reason was that the difference in affinity toward the adsorbent between IC and ATB-2G was less than that between AS-GR and ATB-2G. The reduction in removal efficiency of ATB-2G was more obvious in ternary dye solution because it had the lowest affinity toward the adsorbent among the three dyes.

3.4. Adsorption isotherms in single and mixed dye solutions

The equilibrium adsorption isotherm is important in the design of adsorption systems. Figs. 6 and 7 illustrate the adsorption isotherms of the three dyes in single, binary and ternary dye systems. The shape of the isotherms was related to the type of dye and the components of the solutions. In adsorption from single dye solutions, the isotherms rose steeply at low liquid phase concentration indicating completion adsorption with a plateau formed when the maximum adsorption capacity was achieved. This result revealed that the number of adsorption sites available for dyes on PDADMA–bentonite was limited, and that a saturation adsorbate monolayer was established. The isotherms of individual dye in the binary and ternary dye systems had less regular shape than normal L-type isotherm. In adsorption from binary dye solution of AS-GR + ATB-2G, the reduction of the amounts of ATB-2G adsorbed with increasing equilibrium dye concentration showed clearly the displacement effect by AS-GR molecules from solution. In the ternary dye system, the reduction in the amounts of ATB-2G and IC adsorbed with increasing equilibrium dye concentration was observed in their isotherms.

3.5. Adsorption isotherm models in single and mixed dye solutions

In order to optimize the design of an adsorption system to remove dyes from solutions, it is important to establish the most appropriate correlation for the equilibrium curve. Several models have been used in the literatures to describe the experimental data of adsorption isotherms. The Langmuir model is the most frequently employed model and given by [47]

$$Q_e = \frac{Q_{max} K_L C_e}{1 + K_L C_e} \quad (5)$$

where Q_e is the amount of solute adsorbed at equilibrium (mol/g), C_e is the concentration of adsorbate (mol/L) at equilibrium, Q_{max} (mol/g) and K_L (L/mol) are Langmuir constants related to adsorption capacity and energy of adsorption, respectively.

As illustrated in Table 1, the correlation coefficients, R^2, for the Langmuir isotherm model were greater than 0.999 in single dye systems. This result revealed that the number of adsorption sites on PDADMA–bentonite was limited and that the dye mixtures form a monomolecular layer on the adsorbent at saturation. The value of K_L was in the order of AS-GR >IC > ATB-2G, but the value of Q_{max} was in the order of AS-GR > ATB-2G > IC. It should be noted that the plots of the total amount of dyes adsorbed against the total equilibrium dye concentration were well fitted by the Langmuir equation (Table 1). The correlation coefficient was in the range of 0.9989–0.9995.

The essential characteristics of the Langmuir isotherm can be expressed by a dimensionless constant called equilibrium parameter, R_L, that is defined by the following equation [48].

$$R_L = \frac{1}{1 + K_L C_0} \quad (6)$$

where C_0 is the initial dye concentration. The nature of the adsorption process to be either unfavourable ($R_L > 1$), linear ($R_L = 1$), favourable ($0 < R_L < 1$) or irreversible ($R_L = 0$). For an initial dye concentration of 100 μmol/L, the calculated R_L values were in the range of 0.0017–0.026 in the present adsorption processes. This fact revealed that the adsorption processes were favourable.

Table 1
Fitting constants and coefficients of correlation (R^2) for the fits of the Langmuir equations to the experimental data for dye adsorption by PDADMA–bentonite.

Dye	K_L (L/μmol)	Q_{max} (μmol/g)	R^2	R_L
ATB-2G	0.372 ± 0.027	176.3 ± 9.1	0.9993	0.0262
AS-GR	4.31 ± 0.29	228.7 ± 12.4	0.9996	0.00231
IC	0.629 ± 0.042	149.2 ± 8.3	0.9995	0.0156
AS-GR in AS-GR + IC	5.17 ± 0.48	238.9 ± 15.6	0.9987	0.00193
IC in AS-GR + IC	0.753 ± 0.108	183.6 ± 17.3	0.9984	0.0131
AS-GR + IC	0.991 ± 0.064	218.7 ± 9.6	0.9990	0.00999
ATB-2G in AS-GR + ATB-2G	0.623 ± 0.071	191.1 ± 16.4	0.9988	0.0158
AS-GR in AS-GR + ATB-2G	5.84 ± 0.39	236.2 ± 12.5	0.9990	0.00171
AS-GR + ATB-2G	0.878 ± 0.051	221.8 ± 9.5	0.9995	0.0113
ATB-2G in ATB-2G + IC	0.617 ± 0.107	198.2 ± 13.3	0.9985	0.0159
IC in ATB-2G + IC	0.786 ± 0.112	175.5 ± 11.4	0.9984	0.0126
ATB-2G + IC	0.704 ± 0.064	184.8 ± 8.9	0.9989	0.0140
ATB-2G in ternary dye system	0.547 ± 0.093	185.6 ± 15.4	0.9986	0.0180
AS-GR in ternary dye system	5.28 ± 0.49	241.6 ± 11.8	0.9989	0.00189
IC in ternary dye system	0.874 ± 0.157	174.1 ± 13.4	0.9988	0.0113
ATB-2G + IC + AS-GR	0.649 ± 0.048	209.8 ± 9.4	0.9990	0.0152

As mentioned above, the adsorption isotherms of the three dyes were the Langmuir type in single dye solutions while the isotherm of an individual dye in mixed dye solutions had less regular shape than normal L-type isotherm. In this work, an extended Langmuir model [49] in Eq. (7) was employed to fit the experimental data.

$$Q_{ej} = \frac{K_{Lj} Q_{max\,j} C_{ej}}{1 + \sum K_{Lj} C_{ej}} \tag{7}$$

where K_{Lj} is the adsorption equilibrium constant of dye j in mixed dye system.

In adsorption from binary dye solutions, the amounts of dye adsorbed were expressed as

$$Q_{e1} = \frac{K_{L1} Q_{max\,1} C_{e1}}{1 + K_{L1} C_{e1} + K_{L2} C_{e2}} \tag{8-1}$$

$$Q_{e2} = \frac{K_{L2} Q_{max\,2} C_{e2}}{1 + K_{L1} C_{e1} + K_{L2} C_{e2}} \tag{8-2}$$

According to Eqs. (8-1) and (8-2), we have

$$\frac{K_{L2} C_{e2}}{K_{L1} C_{e1}} = \frac{Q_{max\,1} Q_{e2}}{Q_{e1} Q_{max\,2}} \tag{9}$$

After rearrangement, a linear form of the expanded Langmuir model in binary dye system was obtained.

$$\frac{C_{e1}}{Q_{e1}} = \frac{1}{K_{L1} Q_{max\,1}} + \frac{C_{e1}}{Q_{max\,1}} + \frac{Q_{e2} C_{e1}}{Q_{e1} Q_{max\,2}} \tag{10}$$

According to Eq. (10), the values of C_{e1}/Q_{e1} had linear correlation with C_{e1} and $C_{e1}Q_{e2}/Q_{e1}Q_{max2}$ if the adsorption obeyed the expanded Langmuir model. By using Eq. (10) as the fitting model, the isotherm parameters of an individual dye in the binary dye solutions were estimated and listed in Table 1. It can be seen that the isotherms of an individual dye in the binary dye systems followed the expanded Langmuir model. The correlation coefficients were in the range of 0.9984–0.9990.

Similarly, a linear form of the expanded Langmuir model in the ternary dye solution was given by.

$$\frac{C_{e1}}{Q_{e1}} = \frac{1}{K_{L1} Q_{max\,1}} + \frac{C_{e1}}{Q_{max\,1}} + \frac{Q_{e2} C_{e1}}{Q_{e1} Q_{max\,2}} + \frac{Q_{e3} C_{e1}}{Q_{e1} Q_{max\,3}} \tag{11}$$

By using Eq. (11) as the fitting model, the isotherm parameters of the three dyes in the ternary dye solution were estimated and listed in Table 1. The correlation coefficients were greater than 0.998. Comparing with the data in single dye systems, the adsorption equilibrium constants and saturation amounts adsorbed of a dye in mixed dye systems increased slightly.

3.6. Adsorption kinetics in single and mixed dye solutions

Fig. 8 shows the effect of the contact time on the amounts of dyes adsorbed in single dye systems. The adsorption was rapid in the initial stage since there were many available sites for adsorption on the adsorbent and a high concentration of dye molecules in solution. As the dye molecules were adsorbed onto the adsorbent surface, fewer sites were available and the concentration of dye in solution decreased. This reduced adsorption rate, particularly toward the end, suggested the formation of a monolayer of dye molecules on the surface of the adsorbent. In addition, the contact time to approach a stable adsorption amount was shortened under larger dosage of PDADMA–bentonite.

Figs. 9 and 10 depict the kinetic curves of dyes in binary and ternary dye systems. It can be seen that the shape of the kinetic curves was related to the dosage of absorbent. Under the dosage of 0.5 g/L, desorption of adsorbed IC by the replacement of AS-GR from solution was observed. The result revealed that the adsorption included two steps and the competitive adsorption occurred in the mixed AS-GR and IC solution. In the initial stage of sorption, a large number of vacant surface sites were available for adsorption. Hence, the amounts of AS-GR and IC adsorbed were increased

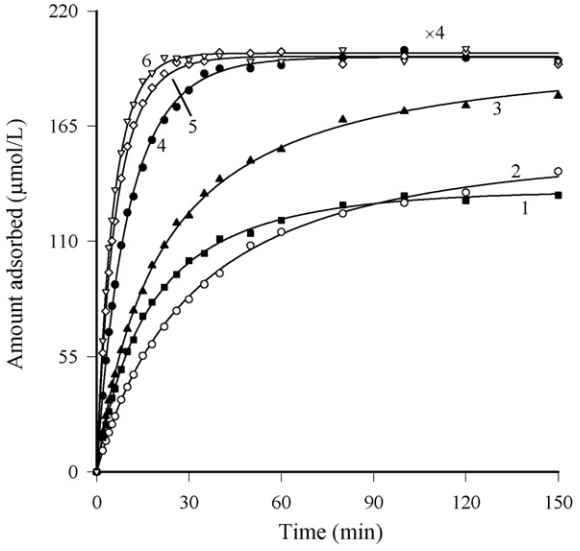

Fig. 8. Effect of contact time on the amounts of dye adsorbed onto PDADMA–bentonite from single dye solutions. (1) and (6) IC; (2) and (4) ATB-2G; (3) and (5) AS-GR. The initial dye concentration was 100 μmol/L and the dosage were 0.5 and 2 g/L in curves 1–3 and 4–6, respectively.

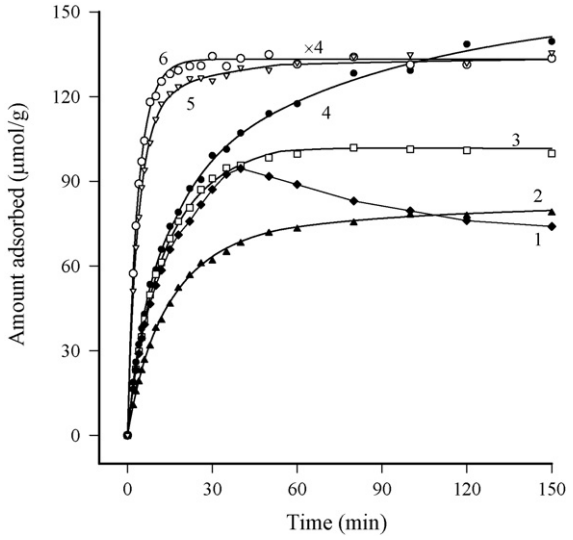

Fig. 9. Effect of contact time on the amounts of dye adsorbed onto PDADMA–bentonite from binary dye solutions. (1) and (6) IC in AS-GR + IC; (2) ATB-2G in ATB-2G + IC; (3) IC in ATB-2G + IC; (4) and (5) AS-GR in AS-GR + IC. The initial dye concentration was 100 μmol/L for each dye and the dosage were 0.5 and 3 g/L in curves 1–4 and 5–6, respectively.

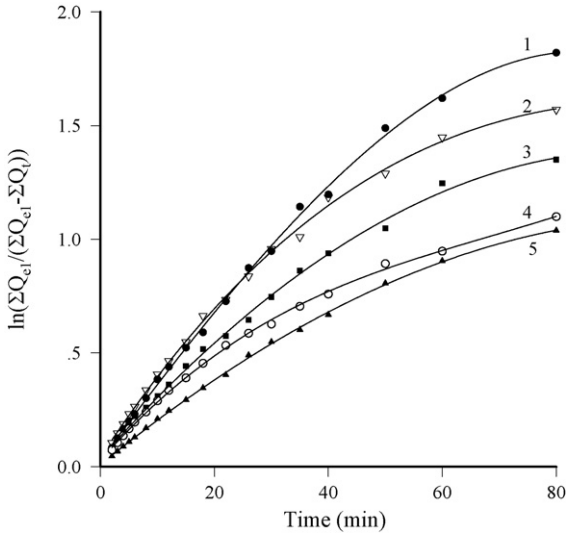

Fig. 11. Pseudo-first-order kinetics for dye adsorption onto PDADMA–bentonite from single dye and mixed solutions. (1) AS-GR; (2) AS-GR + ATB-2G + IC; (3) IC; (4) ATB-2G + IC; and (5) ATB-2G. The dose of PDADMA–bentonite was 1.0 g/L and the initial dye concentration was 100 μmol/L for each dye.

quickly. After lapse of some time, the dye molecules were adsorbed onto the adsorbent that got almost saturation with dye ions. As the adsorption equilibrium constant of AS-GR was greater than that of IC, part of IC molecules previously adsorbed on PDADMA–bentonite were replaced by AS-GR molecules from solution. Consequently, the adsorbed amount of AS-GR increased while adsorbed amount of IC reduced during the stage of the rearrangement of the adsorption layer. Because the difference in adsorption equilibrium constants of IC and ATB-2G was slight, the desorption was not seen in the kinetic curves measured in mixed solution of IC and ATB-2G. As the value of K_L was in the order of AS-GR > IC > ATB-2G, the desorption of IC and ATB-2G occurred in adsorption process from the ternary dye system. Under the dosage of 3 g/L, the competitive adsorption was weakened as there were enough available surface sites for adsorption. Hence, the amounts of dyes adsorbed were increased rapidly in the initial stage and approached to similar stable levels due to low dye concentration in solution.

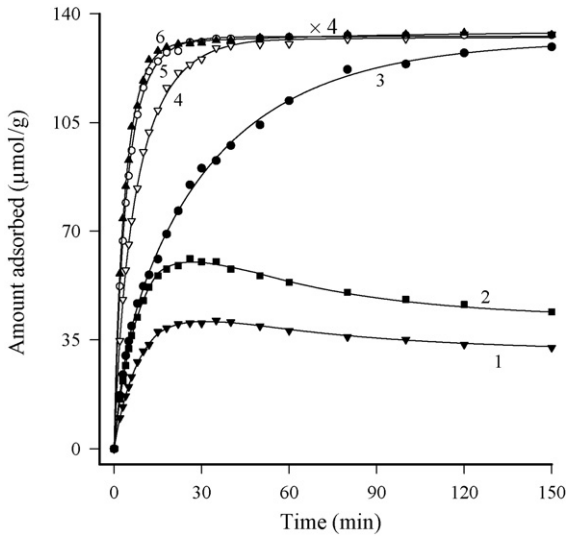

Fig. 10. Effect of contact time on the amounts of dye adsorbed onto PDADMA–bentonite from ternary dye solution. (1) and (4) ATB-2G; (2) and (6) IC; (3) and (5) AS-GR. The initial dye concentration was 100 μmol/L for each dye and the dosage were 0.5 and 3 g/L in curves 1–3 and 4–6, respectively.

3.7. Adsorption kinetics model analysis for dyes onto PDADMA–bentonite

It is important to be able to predict the rate at which contamination is removed from aqueous solutions in order to design an adsorption treatment plant. As seen in Fig. 8, the adsorption processes in single dye solutions were quite rapid and most of the dyes were adsorbed within the first 0.5–1 h of contact. In this work, two kinetic models were employed to fit the experimental data. The first one was the pseudo-first-order kinetic model and the integral form of this model was expressed by the following equation [50]

$$\ln(Q_{e1} - Q_t) = \ln Q_{e1} - k_1 t \quad (12)$$

where Q_{e1} and Q_t are the amounts of dye adsorbed (mol/g) on the adsorbent at the equilibrium and at time t, respectively, k_1 is the rate constant of pseudo-first-order model (min^{-1}); and t is the contact time (min).

Fig. 11 illustrates the correlations of $\ln[Q_{e1}/(Q_{e1} - Q_t)]$ versus t in adsorption from single and mixed dye solutions. In adsorption from mixed dye solutions, the total amounts of dyes adsorbed were used in data treatment. The values of Q_{e1} were amounts of dyes adsorbed after a contact time of 4 h. In addition, only the data in the first 30 min were used because the value of $\ln[Q_{e1}/(Q_{e1} - Q_t)]$ was sensitive to the error in Q_t in the case of $Q_t \approx Q_{e1}$. It can be seen that the plots of $\ln[Q_{e1}/(Q_{e1} - Q_t)]$ against t did not give straight lines.

As listed in Table 2, the correlation coefficient values were greater than 0.99 only in the adsorption from single dye solutions with low dose of PDADMA–bentonite. But the correlation coefficients changed in the range of 0.897–0.989 for total amounts of dyes adsorbed onto PDADMA–bentonite from mixed dye solutions. It should be noted that a higher correlation coefficient could be obtained if the fitting analyses was made in shorter contact time range in the initial stage of adsorption. This result indicated that the experimental data did not agree with the pseudo-first-order kinetic model.

The second model was the pseudo-second-order kinetic model and the integral form of this model was expressed by the following

Table 2
Regressed kinetics parameters for adsorption of dyes from single, binary and ternary dye systems.

Dye	Dose (g/L)	Pseudo-first-order model, t = 2–30 min			Pseudo-second-order model, t = 2–80 min			
		k_1 (min^{-1})	Q_{e1} (μmol/g)	R^2	k_2 (g/mol min)	Q_{e2} (μmol/g)	R^2	h (μmol/g min)
AS-GR	0.5	0.0327	194.7	0.9916	239	206.1	0.9993	10.2
	1.0	0.0721	99.7	0.9961	896	113.9	0.9974	11.6
	2.0	0.1088	49.9	0.9850	6.17×10^3	52.9	0.9978	17.3
	3.0	0.1147	33.3	0.9733	1.49×10^4	34.3	0.9990	24.4
IC	0.5	0.0452	133.9	0.9941	379	153.4	0.9988	8.92
	1.0	0.0547	96.5	0.9898	786	112.6	0.9995	9.96
	2.0	0.1327	49.5	0.9866	4.62×10^3	53.2	0.9979	13.1
	3.0	0.1983	33.1	0.9874	1.02×10^4	34.4	0.9988	17.9
ATB-2G	0.5	0.0266	151.2	0.9959	172	175.7	0.9990	5.31
	1.0	0.0404	96.5	0.9923	421	119.2	0.9983	5.98
	2.0	0.0850	49.4	0.9913	2.07×10^3	56.4	0.9966	6.58
	3.0	0.1222	33.1	0.9905	6.46×10^3	35.7	0.9970	8.23
AS-GR + IC	0.5	0.0496	229.1	0.9877	337	236.2	0.9991	18.8
	1.0	0.0486	190.5	0.9813	526	198.4	0.9996	20.7
	2.0	0.0987	102.0	0.9815	2.26×10^3	108.2	0.9990	26.4
	3.0	0.1119	68.9	0.9761	6.92×10^4	70.7	0.9995	34.6
ATB-2G + AS-GR	0.5	0.0495	216.9	0.9915	284	235.1	0.9988	15.7
	1.0	0.0440	188.7	0.9889	426	196.7	0.9995	16.5
	2.0	0.0922	99.4	0.9867	1.73×10^3	107.8	0.9987	20.1
	3.0	0.1580	66.4	0.9846	5.41×10^3	69.7	0.9988	26.3
ATB-2G + IC	0.5	0.0600	179.9	0.9912	396	206.3	0.9972	16.8
	1.0	0.0456	170.4	0.9892	468	181.0	0.9994	15.3
	2.0	0.0838	99.1	0.9906	1.52×10^3	108.1	0.9987	17.8
	3.0	0.1340	66.3	0.9892	4.69×10^3	70.1	0.9987	23.0
ATB-2G + AS-GR + IC	0.5	0.0749	209.8	0.9901	530	225.5	0.9982	26.9
	1.0	0.0683	197.8	0.9887	575	219.6	0.9993	27.7
	2.0	0.0723	148.1	0.9879	1.078×10^3	162.1	0.9996	28.3
	3.0	0.1236	99.6	0.9851	3.29×10^3	104.7	0.9991	36.1

equation [51]

$$\frac{t}{Q_t} = \frac{1}{k_2(Q_{e2})^2} + \frac{t}{Q_{e2}} \tag{13}$$

where k_2 is the rate constant of the pseudo-second-order model (g/mol min). Q_{e2} is the equilibrium amount of dye adsorbed. The initial rate of adsorption h is

$$h = k_2 Q_{e2}^2 \tag{14}$$

As shown in Fig. 12, the plots of t/Q_t against t gave straight lines. Hence, the values of k_2 and Q_{e2} were determined experimentally from the slope and intercept of the plot of t/Q_t versus t. The regressed kinetics parameters in the pseudo-second-order model for adsorption of dyes from single, binary and ternary dye systems are summarized in Table 2. The correlation coefficients were greater than 0.9966. Therefore, it was ascertained from a comparison of the predicted (best fitted) time dependencies with the experimental data that the pseudo-second-order kinetic equation described the dye adsorption processes more accurately, especially for longer time periods. As can be seen in Table 2, the values of k_2 and h increased with increasing the dosage of PDADMA–bentonite. In adsorption from mixed dye solutions, the values of k_2 and h were greater than those in single dye system due to larger total initial dye concentration. In addition, the values of Q_{e2} obtained from the regression calculation were slightly larger than the experimental values of Q_{e1}.

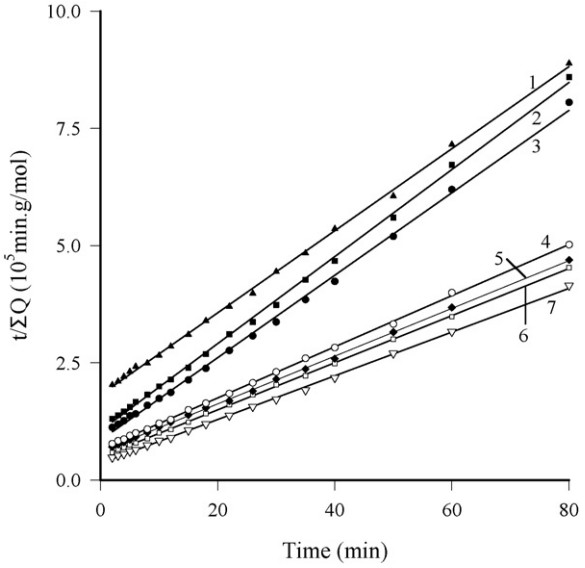

Fig. 12. Pseudo-second-order kinetics for dye adsorption onto PDADMA–bentonite from single dye and mixed solutions. (1) ATB-2G; (2) IC; (3) AS-GR; (4) ATB-2G + IC; (5) AS-GR + ATB-2G; (6) AS-GR + IC; and (7) AS-GR + ATB-2G + IC. The dose of PDADMA–bentonite was 1.0 g/L and the initial dye concentration was 100 μmol/L for each dye.

4. Conclusions

This work indicated that PDADMA–bentonite can be used as a low-cost adsorbent for treating simulated wastewaters of anionic dyes. In the adsorption in single dye solutions, the adsorption isotherms of AS-GR, IC and ATB-2G onto PDADMA–bentonite were well described by the Langmuir adsorption equation. In the adsorption from binary and ternary dye solutions, the removal efficiency was higher for the dye that had a greater equilibrium adsorption constant, especially in the insufficient dosage region. Experimental data indicated that competition for the adsorption sites on the PDADMA–bentonite surface resulted in a reduction in the amounts

of dyes absorbed. In adsorption from the ternary dye solution with same initial concentration of each dye, the adsorption efficiencies for the dyes were in the order of AS-GR > IC > ATB-2G at an insufficient dose of PDADMA–bentonite. The desorption of IC and ATB-2G was observed in the kinetic curves in binary and ternary systems. But the total adsorption isotherms from binary and ternary systems were described by the Langmuir isotherm model. The adsorption isotherm of an individual dye in mixed dye solutions followed an expanded Langmuir isotherm model. The adsorption kinetics for the three dyes from single dye systems, and the total amounts of dyes adsorbed from mixed dye systems, followed the pseudo-second-order kinetic equation. The adsorption rate constants were observed to increase with increasing dosage of the PDADMA–bentonite.

Acknowledgements

This work is supported by the Natural Science Foundation of Shandong Province (Y2007B06, Y2008B12), the Natural Science Foundation of China (No.50578089) and Key Projects in the National Science & Technology Pillar Program in the Eleventh Five-year Plan Period (2006BAJ08B05-2).

References

[1] C.I. Pearce, J.R. Lloyd, J.T. Guthrie, The removal of colour from textile wastewater using whole bacterial cells: a review, Dyes Pigments 58 (2003) 179–196.
[2] G. Crini, Low-cost adsorbents for dye removal: a review, Bioresour. Technol. 97 (2006) 1061–1085.
[3] A. Bhatnagar, A.K. Jain, A comparative adsorption study with different industrial wastes as adsorbents for the removal of cationic dyes from water, J. Colloid Interface Sci. 281 (2005) 49–55.
[4] P.C.C. Faria, J.J.M. Drfao, M.F. Pereira, Adsorption of anionic and cationic dyes on activated carbons with different surface chemistries, Water Res. 38 (2004) 2043–2052.
[5] H.Y. Shu, W.P. Hsieh, Treatment of dye manufacturing plant effluent using an annular UV/H_2O_2 reactor with multi-UV lamps, Sep. Purif. Technol. 51 (2006) 379–386.
[6] S.F. Kang, C.H. Liao, S.T. Po, Decolorization of textile wastewater by photo-Fenton oxidation technology, Chemosphere 41 (2000) 1287–1294.
[7] M.S. Lucas, J.A. Peres, Decolorization of the azo dye Reactive Black 5 by Fenton and photo-Fenton oxidation, Dyes Pigments 71 (2006) 236–244.
[8] A.B. dos Santos, F.J. Cervantes, J.B. van Lier, Review paper on current technologies for decolourisation of textile wastewaters: perspectives for anaerobic biotechnology, Bioresour. Technol. 98 (2007) 2369–2385.
[9] M. Kornaros, G. Lyberatos, Biological treatment of wastewaters from a dye manufacturing company using a trickling filter, J. Hazard. Mater. 136 (2006) 95–102.
[10] Y. Fu, T. Viraraghavan, Fungal decolorization of dye wastewaters: a review, Bioresour. Technol. 79 (2001) 251–262.
[11] J.H. Choi, W.S. Shin, S.H. Lee, D.J. Joo, J.D. Lee, Application of synthetic polyamine flocculants for dye wastewater treatment, Sep. Purif. Technol. 36 (2001) 2945–2958.
[12] V. Golob, A. Vinder, M. Simonic, Efficiency of the coagulation/flocculation method for the treatment of dyebath effluents, Dyes Pigments 67 (2005) 93–97.
[13] N. Daneshvar, H.A. Sorkhabi, M.B. Kasiri, Decolorization of dye solution containing Acid Red 14 by electrocoagulation with a comparative investigation of different electrode connections, J. Hazard. Mater. B 112 (2004) 55–62.
[14] C. Suksaroj, M. Heran, C. Allegre, F. Persin, Treatment of textile plant effluent by nanofiltration and/or reverse osmosis for water reuse, Desalination 178 (2005) 333–341.
[15] F. Javier Benytez, J.L. Acero, A.I. Leal, Application of microfiltration and ultrafiltration processes to cork processing wastewaters and assessment of the membrane fouling, Sep. Purif. Technol. 50 (2006) 354–364.
[16] R. Sanghi, B. Bhattacharya, Review on decolorisation of aqueous dye solutions by low cost adsorbents, Color. Technol. 18 (2006) 256–269.
[17] G. Annadurai, L.Y. Ling, J.F. Lee, Adsorption of reactive dye from an aqueous solution by chitosan: isotherm, kinetic and thermodynamic analysis, J. Hazard. Mater. 152 (2008) 337–346.
[18] D.C.K. Ko, D.H.K. Tsang, J.F. Porter, G. McKay, Applications of multipore model for the mechanism identification during the adsorption of dye on activated carbon and bagasse pith, Langmuir 19 (2003) 722–730.
[19] R.M. Gong, M. Li, C. Yang, Y.Z. Sun, J. Chen, Removal of cationic dyes from aqueous solution by adsorption on peanut hull, J. Hazard. Mater. B121 (2005) 247–250.
[20] S.J. Allen, G. Mckay, J.F. Porter, Adsorption isotherm models for basic dye adsorption by peat in single and binary component systems, J. Colloid Interface Sci. 280 (2004) 322–333.
[21] R.P. Han, D.D. Ding, Y.F. Xu, W.H. Zou, Y.F. Wang, Y.F. Li, L.N. Zou, Use of rice husk for the adsorption of Congo red from aqueous solution in column mode, Bioresour. Technol. 99 (2008) 2938–2946.
[22] N. Dizge, C. Aydiner, E. Demirbas, M. Kobya, S. Kara, Adsorption of reactive dyes from aqueous solutions by fly ash: kinetic and equilibrium studies, J. Hazard. Mater. 150 (2008) 737–746.
[23] R. Jain, S. Sikarwar, Removal of hazardous dye Congo red from waste material, J. Hazard. Mater. 152 (2008) 942–948.
[24] Q.H. Hu, S.Z. Qiao, F. Haghseresht, M.A. Wilson, G.Q. Lu, Adsorption study for removal of basic red dye using bentonite, Ind. Eng. Chem. Res. 45 (2006) 733–738.
[25] A.H. Gemeay, Adsorption characteristics and the kinetics of the cation exchange of Rhodamine-6G with Na^+-montmorillonite, J. Colloid Interface Sci. 251 (2002) 235–241.
[26] M. Özacar, I.A. Sengil, Application of kinetic models to the sorption of disperse dyes onto alunite, Colloids Surf., A 242 (2004) 105–113.
[27] M. Dogan, Y. Ozdemir, M. Alkan, Adsorption kinetics and mechanism of cationic methyl violet and methylene blue dyes onto sepiolite, Dyes Pigments 75 (2007) 701–713.
[28] S.K. Alpat, Ö. Özbayrak, S. Alpat, H. Akcay, The adsorption kinetics and removal of cationic dye, Toluidine Blue O, from aqueous solution with Turkish zeolite, J. Hazard. Mater. 151 (2008) 213–220.
[29] M.A.M. Khraisheh, M.A. Al-Ghouti, S.J. Allen, M.N. Ahmad, Effect of OH and silanol groups in the removal of dyes from aqueous solution using diatomite, Water Res. 39 (2005) 922–932.
[30] N.K. Lazaridis, T.D. Karapantsios, D. Georgantas, Kinetic analysis for the removal of a reactive dye from aqueous solution onto hydrotalcite by adsorption, Water Res. 37 (2003) 3023–3033.
[31] Q. Li, Q.Y. Yue, Y. Su, B.Y. Gao, L. Fu, Cationic polyelectrolyte/bentonite prepared by ultrasonic technique and its use as adsorbent for Reactive Blue K-GL dye, J. Hazard. Mater. 147 (2007) 370–380.
[32] A. Özcan, C. Ömeroğlu, Y. Erdoğan, A.S. Özcan, Modification of bentonite with a cationic surfactant: an adsorption study of textile dye Reactive Blue 19, J. Hazard. Mater. 140 (2007) 173–179.
[33] T.S. Anirudhan, M. Ramachandran, Surfactant-modified bentonite as adsorbent for the removal of humic acid from wastewaters, Appl. Clay Sci. 35 (2007) 276–281.
[34] M. Fuller, J.A. Smith, S.E. Burns, Sorption of nonionic organic solutes from water to tetraalkylammonium bentonites: mechanistic considerations and application of the Polanyi–Manes potential theory, J. Colloid Interface Sci. 313 (2007) 405–413.
[35] Y.H. Shen, Removal of phenol from water by adsorption–flocculation using organobentonite, Water Res. 36 (2002) 1107–1114.
[36] P. Baskaralingam, M. Pulikesi, D. Elango, V. Ramamurthi, S. Sivanesan, Adsorption of acid dye onto organobentonite, J. Hazard. Mater. B128 (2006) 138–144.
[37] Q.Y. Yue, Q. Li, B.Y. Gao, Y. Wang, Kinetics of adsorption of disperse dyes by polyepicholorohydrin-dimethylamine cationic polymer/bentonite, Sep. Purif. Technol. 54 (2007) 279–290.
[38] S.L. Tian, L.Z. Zhu, Y. Shi, Characterization of sorption mechanisms of VOCs with organobentonites using a LSER approach, Environ. Sci. Technol. 38 (2004) 489–495.
[39] M. Cruz-Guzmän, R. Celis, M.C. Hermosän, W.C. Koskinen, J. Cornejo, Adsorption of pesticides from water by functionalized organobentonites, J. Agric. Food Chem. 53 (2005) 7502–7511.
[40] Z. Rawajfih, N. Nsour, Characteristics of phenol and chlorinated phenols sorption onto surfactant-modified bentonite, J. Colloid Interface Sci. 298 (2006) 39–49.
[41] R.K. Taylor, Cation exchange in clays and mudrocks by methylene blue, J. Chem. Technol. Biotech. A 35 (1985) 195–207.
[42] Y. Al-Degs, M.A.M. Khraisheh, S.J. Allen, M.N. Ahmad, G.M. Walker, Competitive adsorption of reactive dyes from solution: equilibrium isotherm studies in single and multisolute systems, Chem. Eng. J. 128 (2007) 163–167.
[43] D.L. Yang, W.P. Li, Q. Kang, D.Z. Shen, Influence of light scattering of residual silica particles on the estimation of surfactant adsorption by spectrometry, Colloids Surf., A 227 (2003) 113–123.
[44] Q. Kang, Residual color profiles of simulated reactive dyes wastewater in flocculation processes by polydiallyldimethylammoniumchloride, Sep. Purif. Technol. 57 (2007) 356–365.
[45] G. Kahr, F.T. Madsen, Determination of the cation exchange capacity and the surface area of bentonite, illite and kaolinite by methylene blue adsorption, Appl. Clay Sci. 9 (1995) 327–336.
[46] A. Özcan, Ç. Ömeroğlu, Y. Erdoğan, A.S. Özcan, Modification of bentonite with a cationic surfactant: an adsorption study of textile dye Reactive Blue 19, J. Hazard. Mater. 140 (2007) 173–179.
[47] I. Langmuir, The constitution and fundamental properties of solids and liquids, J. Am. Chem. Soc. 38 (1916) 2221–2295.
[48] S.K. Das, J. Bhowal, A.R. Das, A.K. Guha, Adsorption behavior of Rhodamine B on rhizopus oryzae biomass, Langmuir 22 (2006) 7265–7272.
[49] K.K.H. Choy, J.F. Porter, G. McKay, Langmuir isotherm models applied to multicomponent sorption of acid dyes from effluent onto acticated carbon, J. Chem. Eng. Data 45 (2000) 575–584.
[50] S. Lagergren, Zur theoric der sogenannten adsorption geloster stoffe, K. Sven. Vetenskapsakad. Handl. 24 (4) (1898) 1–39.
[51] G. McKay, Y.S. Ho, Pseudo-second order model for sorption processes, Process Biochem. 34 (1999) 451–465.